Journal of Pharmaceutical and Biomedical Analysis 197 (2021) 113962

Contents lists available at ScienceDirect

Journal of Pharmaceutical and Biomedical Analysis

journal homepage: www.elsevier.com/locate/jpba

Isolation, identification, and HPTLC quantification of dehydrodeoxycholic acid from Persian Gulf sponges

Fereshteh Golfakhrabadi [a], Mostafa Khaledi [b], Melika Nazemi [c], Mehdi Safdarian [d,*]

[a] Department of Pharmacognosy, Medicinal Plant Research Center, Faculty of Pharmacy, Ahvaz Jundishapur University of Medical Sciences, Ahvaz, Iran
[b] Marine Pharmaceutical Science Research Center, Department of Pharmacognosy, Ahvaz Jundishapur University of Medical Sciences, Ahvaz, Iran
[c] Persian Gulf and Oman Sea Ecological Research Organization, Iranian Fisheries Research Organization, Bandar Abbas, Iran
[d] Nanotechnology Research Center, Ahvaz Jundishapur University of Medical Sciences, Ahvaz, Iran

ARTICLE INFO

Article history:
Received 16 November 2020
Received in revised form 5 February 2021
Accepted 6 February 2021
Available online 13 February 2021

Keywords:
Dysidea avara
Axinella sinoxea
Molecular docking
HPTLC
Marine sponge fingerprint
Psoriasis

ABSTRACT

This study aims to investigate the chemical constituents of sponges *Dysidea avara* (*D. avara*) and *Axinella sinoxea* (*A. sinoxea*), grown up in the Persian Gulf, as well as dehydrodeoxycholic acid (DHCA) content in methanolic extracts of the selected sponges. The chromatography-mass spectrometry (GC–MS) fingerprint of bioactive compounds from methanolic extracts of the selected marine sponge samples was investigated. Based on molecular docking results, among chemical compounds found in marine sponges, DHCA has anti-inflammatory and antipsoriatic properties. They also indicated that DHCA generated stable complexes with 1w81, 3bqm, and 3k8o receptors (psoriasis-related targets) with a binding energy (BE) of −9.26, −10.62, and −7.59 kcal mol^{-1}, respectively. DHCA is isolated from the methanolic extracts of marine sponge samples on chromatographic plates was quantified after derivatization with anisaldehyde reagent by the validated HPTLC method. In-situ HPTLC-DPPH was also calculated to evaluate the free radical-scavenging activity (FRSA) of DHCA. In-silico ADME (Absorption, Distribution, Metabolism, Excretion) predictions revealed that the compound had minimum toxicity and acceptable human intestinal absorption (HIA), as well as low skin permeability. These can potentially be employed as lead compounds to develop a novel antipsoriatic drug.

1. Introduction

As the world's earliest and simplest multicellular organisms, sponges are poorly organized [1]. Among them are marine sponges that create secondary (or specialized) metabolites applicable as natural resources to develop novel cosmetic products and medicines [2]. Studies on marine sponges indicated that sponges *D. avara* and *A. sinoxea*, have cytotoxic effects on cancer cell lines and antiproliferative activities. thus, marine drugs are suggested to be potentially used as a beneficial medicine in cancer therapy. Although most researchers have focused on the antileukemic, Antifungal, antiviral, and anticancer [3] properties of sponge extracts, some of their compounds have also been shown to possess antipsoriatic properties [4]. While many studies have been conducted worldwide to evaluate the pharmacological properties of sponge compounds, there are still many unknown compounds in sponges.

Psoriasis (PsO) is among the most common chronic inflammatory skine disease whose global incidence rates are in the range of 0.6–4.8% [5]. Although there are numerous antipsoriatic therapies to improve the patient's health status in the short run and control the disease in the long run, they fail to clear up psoriasis lesions completely [8]. Based on the pathogenesis and treatment of psoriasis using drugs, there are nine target proteins (human source and crystal structure of the complex): Integrin alpha-L (3bqm), Peptidyl-prolyl cis-trans isomerase A (PPIase) (1w81) and Purine nucleoside phosphorylase (PNP) (3k8o), to name a few, highly correlated with psoriasis. A computational study was conducted on the optimized complex structure of target proteins derived from Protein Data Bank (PDB) to discover compounds highly correlated with them [6].

It is even more challenging to control the quality and determine the metabolic compounds to prepare sponges compared to designer drugs due to the chemical complexity of ingredients. Chromatographic techniques, particularly high-performance liquid chromatography (HPLC) and gas chromatography-mass spectrometry (GC–MS) have hitherto been utilized extensively to develop reference sponge fingerprints. They can also be applied

* Corresponding author.
E-mail address: msafdaryan@gmail.com (M. Safdarian).

https://doi.org/10.1016/j.jpba.2021.113962
0731-7085/

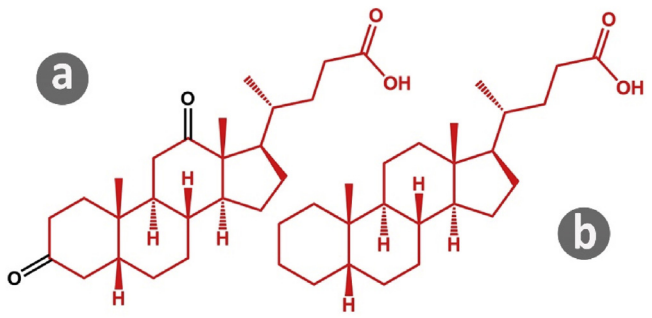

Fig. 1. Chemical structure of a: DHCA and b: 5β-cholan-24-oic acid.

to determine these types of marker compounds quantitatively [7]. However, high-performance thin-layer chromatography (HPTLC) is a logical approach that can be used to carry out both quantitative and qualitative (e.g., fingerprinting, screening) analyses and to further scrutinize plant and marine extracts prior to HPLC analysis [8,9]. HPTLC has been reported to have several advantages, including its capability in simultaneous analyzing various samples, short separation time, and less sample purification-related restrictions (even crude extracts are applicable). It also allows pre- and post-development in-situ analyte derivatization, specifically DPPH (2,2-diphenyl-1-picrylhydrazyl) radical scavenging assay. Furthermore, finite quantities of needful reagents render HPTLC a green analytical tool [10]. In this study, we proposed a valid HPTLC method for the quantitative determination of DHCA in sponge extracts.

It has been discovered that specific bile acids differentially activate four nuclear receptors, namely farnesoid X receptor (FXR), pregnane X receptor (PXR), constitutive androstane receptor, and vitamin D receptor (VDR); besides, one G-protein-coupled receptor (TGR5) has identified bile acids as hormones that alter multiple metabolic pathways in many tissues [11]. Reportedly, the expression of IL-4 in the lesional skin model was selectively reduced, and the frequency of Foxp3+ regulatory T-cells was selectively increased as a result of administering a VDR agonist to mice with allergen-triggered atopic dermatitis (AD) (eczema) [12]. Fig. 1a shows the chemical structure of DHCA, which could be seen in our initial studies on sponges in GC–MS fingerprints. This compound is very similar in structure to unconjugated bile acids, which have 24 carbon atoms with the basic structure of 5β-cholan-24-oic acid (Fig. 1b) [13]. Clinically, treatment with bile acids has been shown to improve psoriasis [14] Accordingly, this study used in-silico molecular docking to examine the antipsoriatic potential of DHCA.

This study outlines the development of a novel, straightforward, swift, cost-effective, and substantiated HPTLC technique to estimate DHCA in methanolic extracts of two sponges (i.e., *D. avara*, *A. sinoxea*) from the Persian Gulf. GC–MS fingerprints of bioactive compounds from methanolic extracts of the selected marine sponges were also investigated. Moreover, antioxidant properties and in-silico molecular docking, as well as absorption, distribution, metabolism and excretion (ADME), were predicted for target bioactive compound molecules.

2. Materials and methods

2.1. Utilized chemicals

DHCA (3,12-Dioxo-5-beta-cholan-24-oic acid), gallic acid (GA) (3,4,5-trihydroxybenzoic acid), $C_7H_6O_5$), and DPPH (2,2-Di(4-tert-octylphenyl)-1-picrylhydrazyl) were purchased from Sigma-Aldrich (St. Louis, MO, USA). 4-anisaldehyde ($C_8H_8O_2$), ammonia (NH_3), Ethanol (EtOH), ethyl acetate (EtAc, $C_4H_8O_2$), glacial acetic acid (HOAc, CH_3CO_2H), hexane (n-Hex, C_6H_{14}), hydrochloric acid (HCl), and toluene (a.k.a. toluol or methylbenzene, C_7H_8) were purchased from Merck KGaA (Darmstadt, Germany). All of the above are analytical reagent (AR) grade chemicals. One mg/mL of DHCA and 25 mg/mL of stock solutions of crude extracts were prepared in the HPTLC mobile phase and stored in the dark at 4 °C. The stock solutions above are serially diluted to prepare working solutions. Separations were conducted on 20 cm × 10 cm normal-phase (NP) glass HPTLC silica gel 60 F_{254} plates (Merck, Darmstadt, Germany).

2.2. Sample collection and identification

Marine sponges *D. avara* and *A. sinoxea* were collected in December 2018 through scuba diving at a depth of 10–15 m from Hengam Island, Strait of Hormuz, the narrow mouth of the Persian Gulf, Iran (at 55° 54′40″-55° 54′55″ E and 26° 36′43″-26° 41′15″ N). Samples were frozen (−20 °C) and transferred to the laboratory. Taxonomic identification was carried out based on dissociated spicule mounts, light optical microscope, scanning electron microscope (SEM), and skeletal slides according to Hooper identification key [15].

2.3. Preparation of sponge extracts

The samples were initially rinsed in seawater and then swiftly in freshwater to remove all noticeable surface residues. Freshly collected sponge samples were cut into small pieces (1 cm) and then freeze-dried. A weighed quantity of powdered sponge (i.e., 100 g) was fully soaked in a certain quantity of methanol (i.e., 1 L) for 72 h (better extraction efficiency than EtOH and n-Hex based on TLC pre-studies), and the resulting extract was then filtered. Afterward, a rotary vacuum evaporator was used to pool and concentrate the extracts obtained during the whole process at a maximum temperature of 38 °C and then to freeze-dry them (yield-5% and 4% for *D. avara* and *A. sinoxea*, respectively). Crude extracts were kept at −20 °C for later use.

2.4. GC–MS analysis

Prior to GC–MS analysis, extracts were silylated by utilizing N-methyl-N-(trimethylsilyl)trifluoroacetamide (MSTFA) subjected to derivatization. As an effective trimethylsilyl donor, MSTFA reacts with substituted labile hydrogens on numerous polar compounds with the group -Si$(CH_3)_3$, rendering it useful for preparing thermostable, volatile derivatives for GC–MS [16]. In short, the extract (1 mg) was mixed with dichloromethane (DCM) (100 μl), vortexed, and N_2-dried. The remaining solution was mixed with MSTFA (50 μl), heated at 80 °C for 15 min in water baths, sealed with parafilm, and stored at −20 °C until subjected to GC–MS analysis. The samples were analyzed up to 2 h after their derivation.

GC–MS analysis was conducted using Agilent 7890A GC (Agilent, Little Falls, DE, USA) equipped with Agilent 5975C Inert XL Mass Selective Detector (MSD). Volatile organic compounds (VOCs) were separated by HP-5MS (30 m × 0.320 mm; 0.25 μm). The sample (1 μL) was then injected into GC–MS in the split injection mode (split ratio = 20:1). The oven temperature was set and kept constant at 50 °C for 2 min, followed by a 230 °C increase (10 °C/min) and left there for 5 min. It was estimated that the total execution time was 30 min. High-purity helium (flow rate =1.0 mL/min) was selected as the carrier gas. The axillary, detector and injector temperatures were set at 230 °C, 250 °C, and 150 °C, respectively. Instrumentation control and data acquisition were provided by ChemStation software, version 5.51. Compounds were identified using NIST 5.0a and Wiley 7.1 spectral libraries.

2.5. High-performance thin-layer chromatography (HPTLC)

Prior to use, plates were prewashed with a blank run of methanol and activated by oven drying (OD) for 30 min at 110 °C. The separation of DHCA and fingerprinting of sponges were carried out on 20 cm × 10 cm NP glass HPTLC silica gel 60 F_{254} plates. The sample extracts and standards (10 mL) were observed on the plate by utilizing a CAMAG Automatic TLC Sampler (ATS 4) (CAMAG, Muttenz, Switzerland) as 6 mm bands, 10 mm from the lower edge. TLC plates were made in an automatic twin-trough chamber (AMD2, CAMAG) with a mobile phase: toluene: hexane: methanol: Ethyl acetate: Acetic acid (60: 15: 17.5: 5: 2.5) over a developing distance (at 70 mm) in 37 min. The plates developed were hot air-dried for 5 min. They were then scanned at 525 nm using a CAMAG TLC Scanner 3. In the 300−700 nm range, spot spectra were then recorded using a photodiode array (PDA) detector. Chromatograms were documented at 254 and 366 nm. White light was illuminated upon the development and post-chromatographic derivatization (PCD) with DPPH solution or anisaldehyde reagent using a CAMAG TLC Visualizer 2 equipped with a digital camera having a 12-bit charged-coupled device (CCD), which is governed by winCATS software, version 1.4.7.6337.

2.6. Post-chromatographic derivatization (PCD)

The DPPH solution (0.4% w/v) was prepared in methanol and stored in the dark at 2–8 °C. The solution of anisaldehyde reagent was prepared freshly by mixing anisaldehyde with frozen HOAc/concentrated H_2SO_4 solution in methanol (0.5:10:5:85). The resulting colorless solution was then kept in a refrigerator. The plates established were subsequently photographed in the pre- and post-derivatization periods. They were derivatized by immersing an HPTLC plate in the derivatization agent for 5 s. Following anisaldehyde reagent-mediated derivatization, the plates were heated for 10 min at 110 °C before being visualized. The DPPH solution-derivatized plates were kept away from light for 30 min and under a nitrogen atmosphere and then photographed. High-quality images and inter-plate reproducibility were guaranteed by fixing WinCATS image-acquisition parameters. Free ImageJ 1.46 r was used to process HPTLC chromatogram images.

2.7. Method validation

DHCA determination methods were validated in accordance with the guidelines of the International Conference on Harmonization (ICH) on range and linearity, accuracy, precision, the limit of detection (LOD) and the limit of quantification (LOQ) [24]. To assess the working range, chromatographic peak areas vs. the concentration of standard solutions (μg/ mL) were plotted. The method was assessed for linearity by plotting calibration curves (a.k.a. standard curves) at five concentration levels. Least squares regression analysis (LSRA) was employed in Excel to establish linear ranges. Three repetitions of each standard solution were utilized at three levels of concentration (20, 100, and 200 μg/mL) in the standard curve to assess repeatability. The difference between repetitions was shown as a relative standard deviation (RSD%). The accuracy of the method was evaluated by studying the recovery from the extracted, spiked sponge samples.

Measurement sensitivity was assessed for LOD and LOQ. They were measured using the equation $LOD = 3 \times Sd/B$ and $LOQ = 10 \times Sd/B$, where *Sd* represents the standard deviation from the peak areas of the three blank solutions, used to measure noise, and *B* is the slope of the associated standard curve.

2.8. Molecular docking

Docking was studied by dint of in-house batch script (DOCKFACE) from AutoDock 4.2. For the procedure of docking, each ligand was optimized with molecular mechanics (MM^+) and then semi-empirical method (AM1) based on the Polak-Ribière algorithm, minimization method using HyperChem 8 [17]. Based on the pathogenesis and pharmacological therapy of PsO, target proteins (complex crystal structure and human resource) that are highly correlated with PsO, were selected from the DrugBank database and Therapeutic Targeted Database (TTD) [6].

Table S1 lists three major PsO-related target proteins obtained from the Protein Data Bank (http://www.rcsb.org/pdb/home/home.do). All co-crystal ligands and H_2O molecules in proteins were removed, missing hydrogen atoms were added, and non-polar hydrogens merged with their associated carbons by utilizing AutoDock Tools after assessing the Kollman unified atomic charges. Then, each protein atom was given atomic-based desolvation parameters (ASPs). Proteins were converted to PDBQT format using MGLTOOLS 1.5.6. The molecular docking was performed using a Genetic Algorithm (GA) approach to find the best position of the ligand in the active site of the target protein. the receptor grid maps were calculated using AutoGrid tools of AutoDock 4.2 (Table S1). Cluster analysis was conducted using a tolerance of 2 Å root-mean-square deviation (RMSD) on the docked results. For the internal validation phase, target co-crystal ligands were extracted using a viewer and treated like other ligands [18].

Protein-ligand interactions were assessed using online web-based ProteinsPlus (https://proteins.plus/) [19]. The docking results were evaluated for energy, hydrogen bonding, and hydrophobic interactions between bioactive compounds and targets to evaluate the binding mode of effective inhibitors.

2.9. Pharmacological properties of ADME

The pharmacological properties of DHCA were predicted using pkCSM (http://biosig.unimelb.edu.au/pkcsm) [20] and SwissADME (http://www.swissadme.ch/) [21].

3. Results and discussion

3.1. Sponge identification

Sponges *D. avara* and *A. sinoxea* were identified based on the Hooper identification key.

3.2. Gas chromatography-mass spectrometry (GC–MS)

Compounds were identified by comparing the mass spectrum of the unknown component with spectra of known components stored in the NIST 5.0a and Wiley 7.1 spectral libraries. The GC–MS chromatograms of the extract are shown in Fig. S1 (available in Electronic Supplementary Information, ESI†), indicating the existence of several peaks. using GC–MS, 81 (*A. Sinoxea*) and 68 (*D. avara*) chemical components were identified in marine sponge extracts. Tables S2 (ESI†) shows the identified compounds in the two extracts. As can be seen, DHCA is present in both sponge extracts, whose relative value is greater in *D. avara* (0.81%) than *A. Sinoxea* (0.36%). Instead, the amount of ingredients in sponge *A. Sinoxea* extract is greater than sponge *D. avara*. Consequently, it would be illogical to compare the amount of DHCA through the percentage peak area. The following valid HPTLC method is suggested for the quantitative determination of DHCA in sponge extracts.

Table 1
The figure of merit of HPTLC in determining DHCA.

Parameter	Analytical feature
Liner range	20–400 (μg mL^{-1})
Slope	6.5296
Intercept	321.24
R^2	0.9799
LOD	2.07 (μg mL^{-1})
LOQ	6.90 (μg mL^{-1})
Mean Recovery (n = 6)	99.48 ± 3.55
RSD% (n = 6)	5.85
Repeatability	
20[a]	19.73 ± 2.23[b] (11.30)
100[a]	98.93 ± 5.55[b] (5.61)
200[a]	204.62 ± 4.31[b] (2.11)
Intermediate precision	
20[a]	20.54 ± 1.54[b] (7.49)
100[a]	99.45 ± 3.74[b] (3.75)
200[a]	205.11 ± 3.70[b] (1.80)

[a] Concentration of DHCA added, and [b] concentration found in μg/mL, mean ± SD (RSD%).

3.3. HPTLC analysis of DHCA

In achieving a desirable separation in HPTLC determination, the type and composition of the developing solvent (mobile phase) is an important challenge. The TLC mobile phase is generally selected empirically using existing literature to separate the desired analytes. In this paper, to optimize developing solvents, aluminum plates (2 cm × 7 cm) coated with TLC silica were observed with extracts and DHCA stock solutions. The plates were generated individually by various solvent mixtures (no data are available). Whether DHCA spots exist on the plates are assessed, and the optimal solvent mixture is selected for subsequent HPTLC analyses. Further evaluation of the resolution for DHCA separation suggested toluene: hexane: methanol: ethyl acetate: acetic acid (60:15:17.5:5:2.5) as the optimal solvent mixture in HPTLC analysis of DHCA.

Fig. 2 illustrates DHCA calibration spots in the range of 20–400 μg mL^{-1}, as well as the HPTLC fingerprint profiles of sponge extracts. As can be seen in Fig. 2b, several distinct fingerprint patterns of sponges were observed. Apart from identifying components, the difference in the separation pattern is well seen in the two types of sponges. This HPTLC fingerprint is reproducible for each sponge extract in different concentrations (see samples 3 and 4 in Fig. 2b). The DHCA zone is isolated from other compounds of sponge extracts and is clearly seen in Rf = 0.61 at the same position as standard spots (samples 5–9 in Fig. 2c).

The selected mobile phase gave an excellent resolution of DHCA and reproducible peak at an Rf value of 0.61 (Fig. 3a). The calibration curve (Fig. 3b) for DHCA after derivatization with anisaldehyde reagent was linear in the range of 20–400 μg/mL with the correlation coefficient (R^2) of 0.9799.

The above method was relatively selective with high baseline resolution. The spectra of the spots of the standards and extracts were compared over the range of 300–700 nm, and proper peak priority was observed in the separation of DHCA (data not reported). According to Table 1, the system accuracy, appropriateness, linearity, LoD, LoQ, and precision were examined in accordance with the ICH guidelines. Measurement repeatability was determined by analyzing 20, 100, and 200 μg/mL DHCA three times with the same plate on the same day. On three different days, within-lab reproducibility was defined for the three concentrations above. The results illustrated in Table 1 indicate very high repeatability and reproducibility. A low RSD% indicated that the above method was robust.

The selected HPTLC method was used to analyze DHCA in the methanolic extracts of *D. avara* and *A. Sinoxea*. Using this method, the quantity of DHCA in the methanolic extracts of *D. avara* and *A. Sinoxea* was found to be 156 and 69 mg/g of dried extracts, respectively.

3.4. HPTLC-DPPH analysis

Total antioxidant capacity (TAC) was usually determined by spectrophotometric assays, including free radical-scavenging activity by free radicals of DPPH rather than antioxidant activity of separate components in the extract. As seen in Fig. 4, the HPTLC-DPPH assay was applied to directly screen the antioxidant activity of isolated chromatographic regions under similar chromatographic conditions. DPPH is a deep-purple, stable free radical that turns yellowish when its concentration is reduced by available antioxidants in the sample. Consequently, antioxidants present in the sample turns into yellow or pale yellow spots against a purple background of the plate [22].

A comparison was made between the size of the area and color intensity of yellow bands and the color intensity of yellow bands achieved from gallic acid stock solutions upon being sprayed by the ethanolic solution of DPPH to express FRSA degree in the extracts in gallic acid equivalents (GAEs). The regression equation and correlation coefficient (R^2) of gallic acid with DPPH were obtained as Y = 28.546X+3314.1 and 0.9786, respectively, in 0.2–10.0 μg $Spot^{-1}$ linearity range. LoD (0.06 μg/Spot) and LoQ (0.20 μg/Spot) were calculated to determine the method sensitivity.

Predictably, in accordance with DPPH reagent-mediated detection (Fig. 4c), several discrepancies were spotted in the qualitative HPTLC-DPPH profiles of the extracts obtained from *A. Sinoxea* and *D. avara*. Nevertheless, in track 8 of *A. Sinoxea* (Fig. 4c), there are three active regions with Rf values of 0.53, 0.71 and 0.92 (the most intensified common region) in which different-colored red bands show up at 366 nm before DPPH reagent-mediated derivatization (Fig. 4b). Although these compounds were not identified in this study, their antioxidant properties are evident and can be identified in the future by HPTLC-MS/MS analysis. Compared to sponge *A. Sinoxea*, *D. avara* generally has low antioxidant properties (Table S3).

3.5. Docking analysis

In-silico docking analysis was performed to determine the inhibitory capacity of DHCA as a ligand present in the sponge extracts against the selected psoriasis receptors. The docking analysis results involve the predicted value of binding free energy (ΔGbind) for the optimal position of bound DHCA (kcal/mol) along with associated interactions with essential amino-acid residues. DHCA showed binding energy values of -9.26, -10.62, and -7.59 kcal mol^{-1} with docked 1w81, 3bqm, and 3k8o, respectively (Table 2). In order to adequately compare the efficiency of smaller size ligands with larger size ligands, the ligand efficiency index can be simply calculated using the Eq. 1 [23]:

$$LE = \frac{-\Delta G}{HAC} \quad (1)$$

HAC stands for heavy atom count. When taking all LEs into account, we observed that the best (−ΔG/HAC) efficiency index for DHCA was obtained for Integrin alpha-L (LE = 0.379). Binding interactions of DHCA with 1w81, 3bqm, and 3k8o [6] are shown in Fig. 5. To verify the procedure of docking, co-crystal ligand in PDB of (3R)-1-acetyl-3-methylpiperidine ($C_8H_{15}NO$) (1P3), 3-({4-[(1E)-3-morpholin-4-yl-3-oxoprop-1-en-1-yl]-2,3-bis(trifluoromethyl)phenyl}sulfanyl)aniline ($C_{21}H_{18}F_6N_2O_2S$) (BQM), and 7-({[(1 *r*,2 *s*)-2,3-dihydroxy-1-(hydroxymethyl)propyl]amino}methyl)-3,5-dihydro-4h-pyrrolo[3,2-*d*]pyrimidin-4-one ($C_{11}H_{16}N_4O_4$)

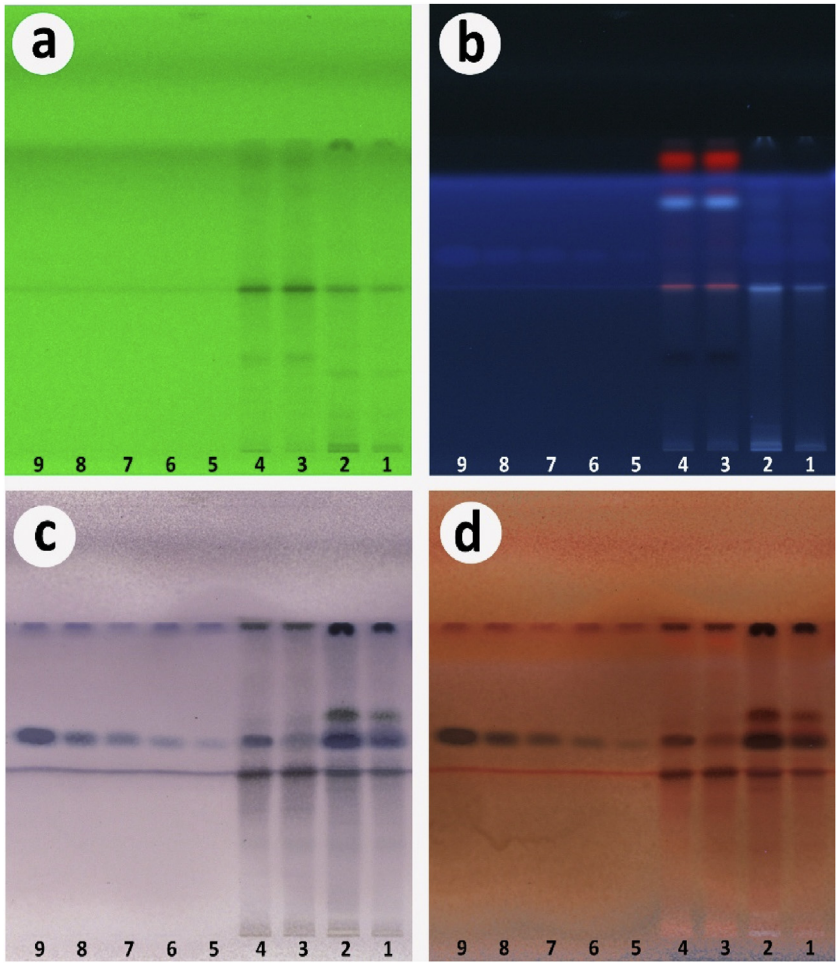

Fig. 2. Pre-derivatization HPTLC fingerprints of sponge extracts (samples 1 and 2, 2.5 and 5 mg/mL from *D. avara* and samples 3 and 4, at the same concentration from *A. Sinoxea,* dried extracts) and DHCA calibration spots (sample 5-9) on NP HPTLC plates at 254 nm (a) 366 nm (b) and following anisaldehyde reagent-mediated post-chromatographic derivatization under white light above (c) 366 nm (d). Mobile phase: toluene: hexane: methanol: ethyl acetate: acetic acid (60: 15: 17.5: 5: 2.5). Applied 10 μL per band.

Table 2
Values of separation energy, ligand efficiency and key amino acids in the active site of Peptidyl-prolylcis-trans isomerase, Integrin alpha-L, and Purine nucleoside phosphorylase proteins in charge of interactions.

Receptors	Compound name	Parameters						
		BE (kcal/mol)	NHB	AARs (HBs)	NPI	AARs (HPI)	HAC	LE
Peptidyl-prolyl cis-trans isomerase	Co-crystal ligand of 1P3	−4.59	1	Asn102A	1	Met61A	10	0.459
	DHCA	−9.26	1	Lys82A	2	Ala103A, Asn102A	28	0.332
Integrin alpha-L	Co-crystal ligand of BQM	−9.38	1	Glu284B	3	Tyr257B, Lys287B,Val233B	32	0.293
	DHCA	−10.62	1	Lys287B	6	Ile235B, Glu284B, Leu302B, Lys267B, Val286B, Ile259B	28	0.379
Purine nucleoside phosphorylase	Co-crystal ligand of 229	−7.01	6	Asn243E, Ala116E, Tyr192E, Ser220E, Arg84E, His86E	1	Ala117E	19	0.399
	DHCA	−7.59	2	His257E, Asn151E	3	Pro62E, Arg158Y, Asn151y	28	0.250

BE: Binding Energy, NHB: Number of Hydrogen bonds, AARs: Amino acid residues, HBs: Hydrogen bonds, NHPI: Number of Hydrophobic Interactions, HPI: Hydrophobic Interactions, HAC: heavy atom count, LE: Ligand efficiency.

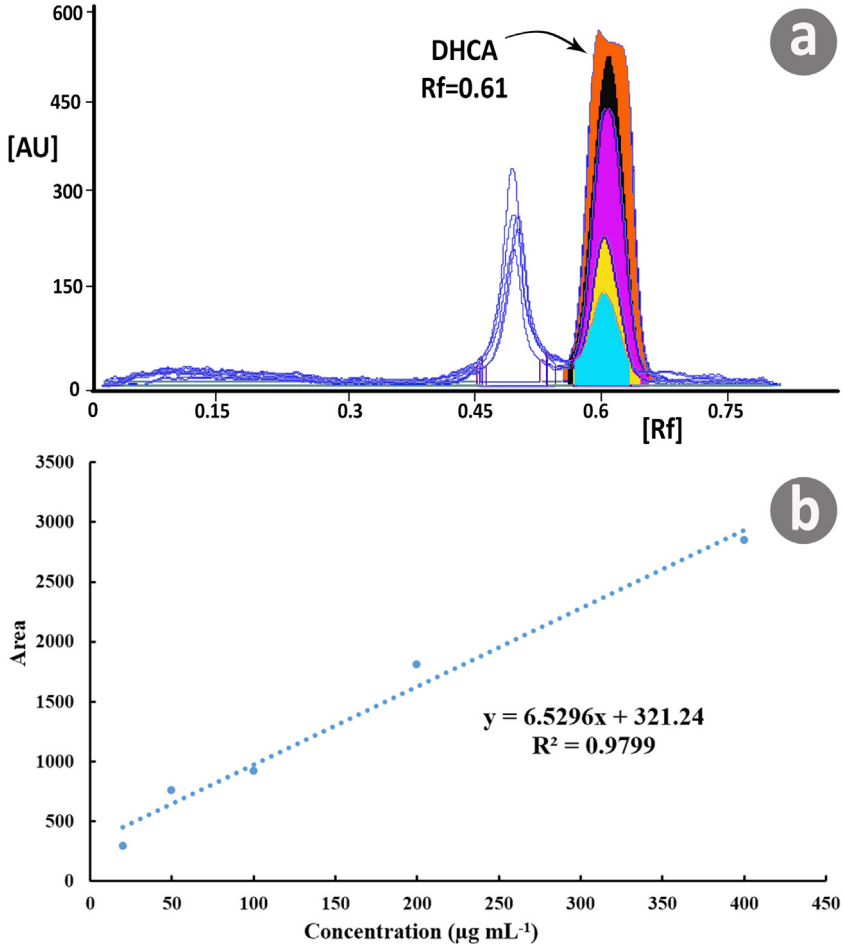

Fig. 3. a: Chromatogram of standard solutions of DHCA after derivatization with anisaldehyde reagent (20-400 µg mL^{-1}) b: Calibration plot of DHCA after derivatization with anisaldehyde reagent (λ_{max} =525 nm). Mobile phase: toluene: hexane: methanol: ethyl acetate: acetic acid (60: 15: 17.5: 5: 2.5).

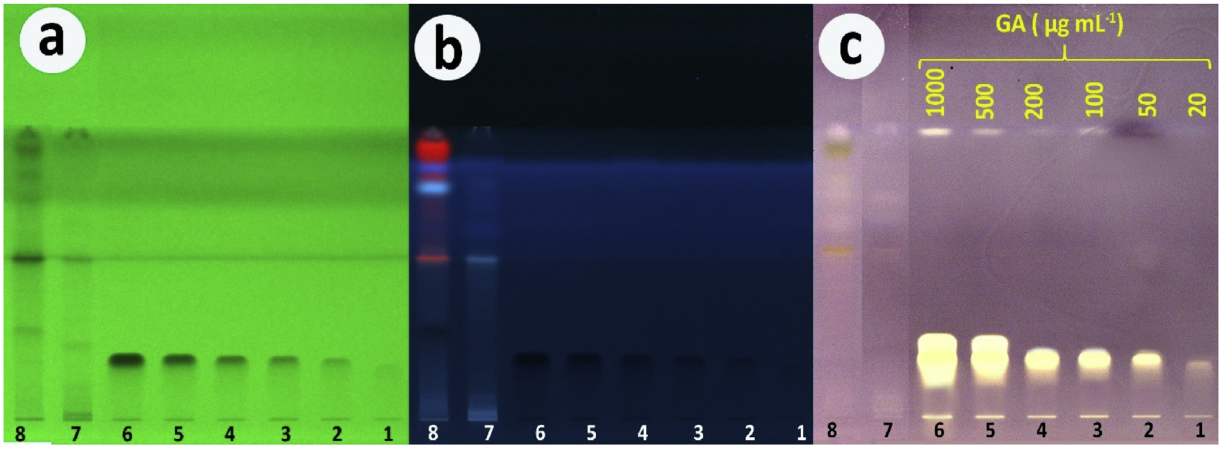

Fig. 4. HPTLC chromatograms of extracts at 254 nm (a), 366 nm (b), after being DPPH-derivatized under white light (c). Mobile phase: toluene: hexane: methanol: ethyl acetate: acetic acid (60:15:17.5:5:2.5). Tracks 1-6, gallic acid standards; tracks 7, *D. avara* extract (10 mg/mL); tracks 8, *A. Sinoxea* extract (10 mg/mL). Applied 10 µL per band.

(229 co-crystal) were extracted and redocked into their targets. The values of RMSD for all targets were less than 2 Å.

Psoriatics often have liver disease and deficiencies in bile acids. Psoriasis is a disease characterized by a leaky gut. All of the comorbidities of this disease are due to systemic endotoxemia. Bacterial peptidoglycans absorbed from the gut have direct toxic effects on the liver and skin. Their absorption, as well as endotoxin absorption, must be eliminated to treat psoriasis successfully. Endotoxin absorption is markedly increased by ethanol and peppers. Bioflavonoids, such as quercetin and citrus bioflavonoids, prevent this absorption. Bile acids, given orally, break up endotoxin in the intestinal lumen [14]. For comparison, the presence of two additional carbonyl groups compared to bile acids can have more effective and stable interactions with essential amino-acid residues. Therefore, in substantiating the initial claim of this study, it should be said that more stable interactions of DHCA with

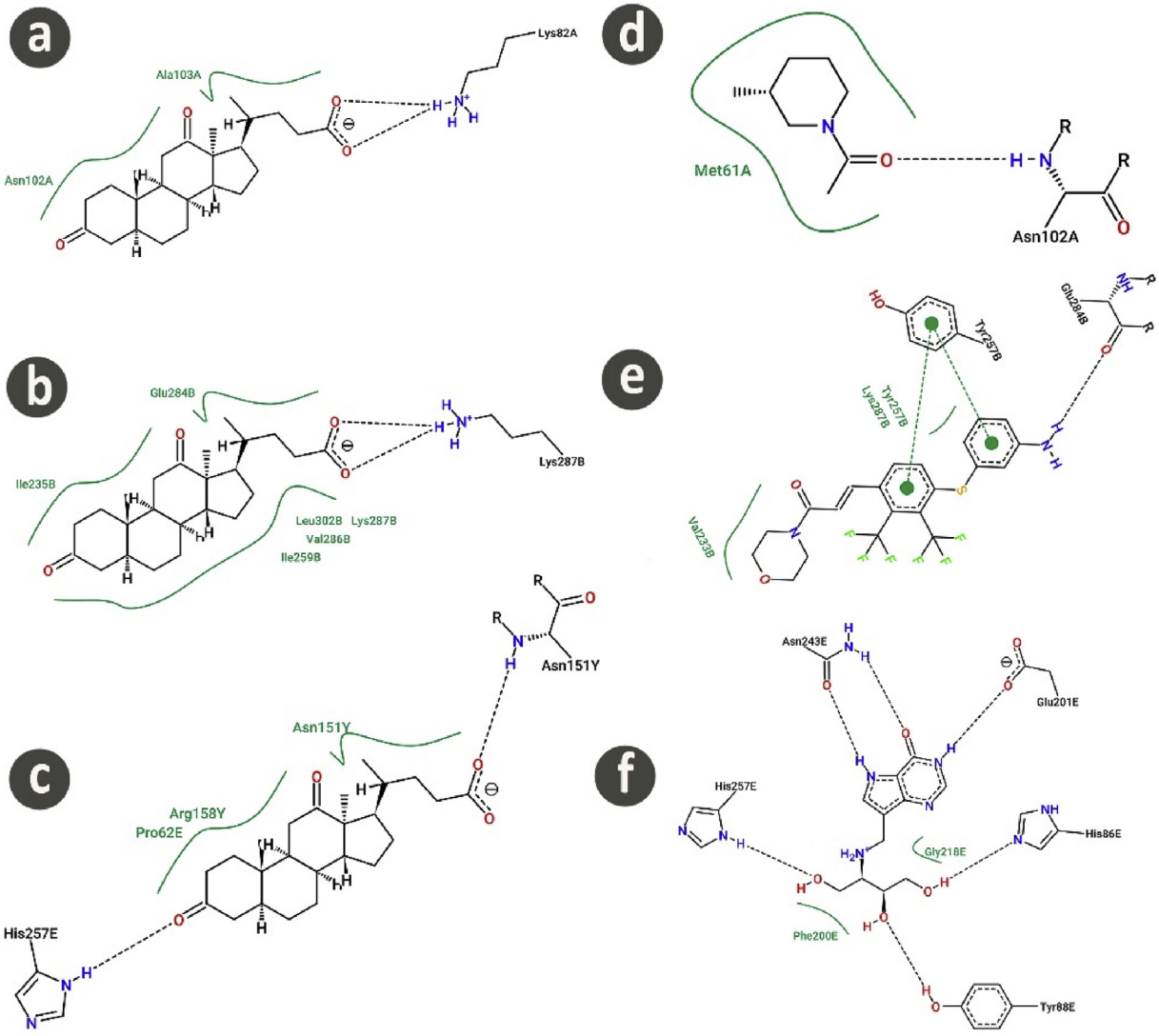

Fig. 5. DHCA docking results within the active site of Peptidyl-prolylcis-trans isomerase (a), Integrin alpha-L (b), and Purine nucleoside phosphorylase (c). Validation of the method by means of docked and crystallized ligand 1P3 (d), BQM (e), and 229 co-crystal (f) (ProteinsPlus).

selected psoriasis receptors will confirm its potent antipsoriatic properties. Cellular and in-vivo studies are required to finally substantiate this claim, which will be conducted by our group in later studies.

3.6. ADME analysis

The ADME properties of a certain compound are determined by its pharmacokinetics and safety profile. ADME behavior is also outshined, usually by toxicity. Small structural changes can significantly effect the pharmacokinetic and toxicity properties of drug candidates. The findings of the ADMET study may be used to enhance the pharmacokinetic profile of the compound by changing its chemical structure or constructing an appropriate drug delivery system (DDS). The SwissADME and pkCSM tools use drug-likeness and molecular properties to comprehensively characterize the pharmacokinetic and toxicity properties of DHCA. The molecular and pharmacological properties of DHCA are detailed in Table S4.

DHCA satisfied drug-likeness (Lipinski, Ghose, Veber, Egan, and Muegge). The suitability of the compound that can be a drug candidate was initially evaluated. The toxicity assessment demonstrated that the ligand was non-mutagenic and non-carcinogenic by the AMES test (Table S4). Of all the parameters above, DHCA clearly exhibits high (100%) human intestinal absorption (HIA). Larger HIAs indicate better absorption of the compound by the intestinal tract after oral administration [24]. In assessing metabolism, the rest of the cytochromes showed non-substrate and non-inhibitory through DHCA. DHCA exhibits low skin permeability (Table S4). Speaking of efflux prediction by P-glycoprotein (P-gp), DHCA acts not as a substrate but as a P-gp inhibitor (P-glycoprotein II inhibitor).

4. Conclusions

To the best of our knowledge, this is the first-ever DHCA count estimation in sponge extract with an accurate HPTLC analysis. It has some benefits, such as reduced organic solvent consumption and fewer limitations related to sample purification. Furthermore, according to molecular docking evaluation, DHCA generates a better complex with less binding energy than co-crystals of the three studied target PsO receptors, indicating the potential of this compound for future in-vivo antipsoriatic investigations. Based on ADME investigation, DHCA could portray itself as an outstanding basic drug candidate thanks to its potency, oral bioavailability, non-toxicity, and low skin permeability.

CRediT authorship contribution statement

Fereshteh Golfakhrabadi: Conceptualization, Funding acquisition, Supervision. **Mostafa Khaledi:** Conceptualization, Software, Writing - original draft. **Melika Nazemi:** Resources, Validation. **Mehdi Safdarian:** Methodology, Formal analysis, Visualization, Writing - review & editing, Supervision.

Declaration of Competing Interest

The authors declare that they have no known competing financial interests or personal relationships that could have appeared to influence the work reported in this paper.

Acknowledgments

We would like to gratefully acknowledge the research deputy of Ahvaz Jundishapur University of Medical Sciences who supported this work under grant number MPRC-9812.

Appendix A. Supplementary data

Supplementary material related to this article can be found, in the online version, at doi:https://doi.org/10.1016/j.jpba.2021.113962.

References

[1] W. Müller, R. Zahn, M. Gasić, N. Dogović, A. Maidhof, C. Becker, B. Diehl-Seifert, E. Eich, Avarol, a cytostatically active compound from the marine sponge Dysidea avara, Comp. Biochem. Physiol. Part C Comp. Pharmacol. 80 (1) (1985) 47–52.
[2] S. de Caralt, J. Sanchez-Fontenla, M.J. Uriz, R.H. Wijffels, In situ aquaculture methods for Dysidea avara (Demospongiae, Porifera) in the northwestern Mediterranean, Mar. Drugs 8 (6) (2010) 1731–1742.
[3] E.M. El-Hossary, C. Cheng, M.M. Hamed, A.N. El-Sayed Hamed, K. Ohlsen, U. Hentschel, U.R. Abdelmohsen, Antifungal potential of marine natural products, Eur. J. Med. Chem. 126 (2017) 631–651.
[4] R.M. Andres, M.C. Montesinos, P. Navalon, M. Paya, M.C. Terencio, NF-kappaB and STAT3 inhibition as a therapeutic strategy in psoriasis: in vitro and in vivo effects of BTH, J. Invest. Dermatol. 133 (10) (2013) 2362–2371.
[5] N. Luigi, Epidemiology of psoriasis, Curr. Drug Targets - Inflamm. Allergy 3 (2) (2004) 121–128.
[6] C. Lu, J. Deng, L. Li, D. Wang, G. Li, Application of metabolomics on diagnosis and treatment of patients with psoriasis in traditional Chinese medicine, Biochim. Biophys. Acta 1844 (1 Pt B) (2014) 280–288.
[7] D. Mahdian, M. Iranshahy, A. Shakeri, A. Hoseini, H. Yavari, M. Nazemi, M. Iranshahi, Cytotoxicity evaluation of extracts and fractions of five marine sponges from the Persian Gulf and HPLC fingerprint analysis of cytotoxic extracts, Asian Pac. J. Trop. Biomed. 5 (11) (2015) 896–901.
[8] G. Sadhasivam, A. Muthuvel, A. Pachaiyappan, B. Thangavel, Isolation and characterization of hyaluronic acid from the liver of marine stingray Aetobatus narinari, Int. J. Biol. Macromol. 54 (2013) 84–89.
[9] E. Genin, G. Wielgosz-Collin, J.M. Njinkoue, N.E. Velosaotsy, J.M. Kornprobst, J.P. Gouygou, J. Vacelet, G. Barnathan, New trends in phospholipid class composition of marine sponges, Comp. Biochem. Physiol. B, Biochem. Mol. Biol. 150 (4) (2008) 427–431.
[10] F. Orsini, I. Vovk, V. Glavnik, U. Jug, D. Corradini, HPTLC, HPTLC-MS/MS and HPTLC-DPPH methods for analyses of flavonoids and their antioxidant activity in Cyclanthera pedata leaves, fruits and dietary supplement, J. Liq. Chromatogr. Relat. Technol. 42 (9–10) (2019) 290–301.
[11] T.Q. de Aguiar Vallim, E.J. Tarling, P.A. Edwards, Pleiotropic roles of bile acids in metabolism, Cell Metab. 17 (5) (2013) 657–669.
[12] M. Umar, K.S. Sastry, F. Al Ali, M. Al-Khulaifi, E. Wang, A.I. Chouchane, Vitamin D and the pathophysiology of inflammatory skin diseases, Skin Pharmacol. Physiol. 31 (2) (2018) 74–86.
[13] P. Nair, The Bile Acids: Chemistry, Physiology, and Metabolism, Volume 3, Pathophysiology, Springer Science & Business Media, 2012.
[14] P.H. Ely, Is psoriasis a bowel disease? Successful treatment with bile acids and bioflavonoids suggests it is, Clin. Dermatol. 36 (3) (2018) 376–389.
[15] J.N. Hooper, R.W. Van Soest, Systema porifera, in: A Guide to the Classification of Sponges, Systema Porifera, Springer, 2002, pp. 1–7.
[16] M. Thevis, G. Opfermann, W. Schänzer, N-methyl-N-trimethylsilyltrifluoroacetamide-promoted synthesis and mass spectrometric characterization of deuterated ephedrines, Eur. J. Mass Spectrom. 10 (5) (2004) 673–681.
[17] S. Zare, M. Fereidoonnezhad, D. Afshar, Z. Ramezani, A comparative QSAR analysis and molecular docking studies of phenyl piperidine derivatives as potent dual NK1R antagonists/serotonin transporter (SERT) inhibitors, Comput. Biol. Chem. 67 (2017) 22–37.
[18] M. Fereidoonnezhad, Z. Faghih, A. Mojaddami, A. Sakhteman, Z. Rezaei, A comparative docking studies of dichloroacetate analogues on four isozymes of pyruvate dehydrogenase kinase in humans, Dent 1 (4) (2016) 5.
[19] R. Fahrrolfes, S. Bietz, F. Flachsenberg, A. Meyder, E. Nittinger, T. Otto, A. Volkamer, M. Rarey, ProteinsPlus: a web portal for structure analysis of macromolecules, Nucleic Acids Res. 45 (W1) (2017) W337–W343.
[20] D.E. Pires, T.L. Blundell, D.B. Ascher, pkCSM: Predicting Small-Molecule Pharmacokinetic and Toxicity Properties Using Graph-Based Signatures, J. Med. Chem. 58 (9) (2015) 4066–4072.
[21] A. Daina, O. Michielin, V. Zoete, SwissADME: a free web tool to evaluate pharmacokinetics, drug-likeness and medicinal chemistry friendliness of small molecules, Sci. Rep. 7 (2017) 42717.
[22] J. Wang, Y.D. Yue, F. Tang, J. Sun, TLC screening for antioxidant activity of extracts from fifteen bamboo species and identification of antioxidant flavone glycosides from leaves of Bambusa. Textilis McClure, Molecules 17 (10) (2012) 12297–12311.
[23] R.M. Qasaymeh, D. Rotondo, C.B. Oosthuizen, N. Lall, V. Seidel, Predictive binding affinity of plant-derived natural products towards the protein kinase g enzyme of Mycobacterium tuberculosis (MtPknG), Plants 8 (11) (2019) 477.
[24] C.M. Nisha, A. Kumar, P. Nair, N. Gupta, C. Silakari, T. Tripathi, A. Kumar, Molecular docking and in Silico ADMET study reveals acylguanidine 7a as a potential inhibitor of beta-secretase, Adv. Bioinformatics (2016) (2016), 9258578.